Magnetic field behavior beyond the laser spot

S. R. Goldman and R. F. Schmalz

Citation: Physics of Fluids **30**, 3608 (1987); doi: 10.1063/1.866442
View online: http://dx.doi.org/10.1063/1.866442
View Table of Contents: http://scitation.aip.org/content/aip/journal/pof1/30/11?ver=pdfcov
Published by the AIP Publishing

Magnetic field behavior beyond the laser spot

S. R. Goldman[a] and R. F. Schmalz
Max-Planck-Institut für Quantenoptik, D-8046 Garching, Federal Republic of Germany

(Received 24 February 1987; accepted 13 August 1987)

A self-consistent, analytic solution for the two-dimensional, rotationally symmetric, time varying problem of the interaction of a laser plasma with its self-generated magnetic field has been determined at lateral locations away from the laser spot. The plasma is described by a two-fluid model, with the magnitude of the electron velocity much greater than the ion velocity. Increased spatial gradients in the density and velocity around the magnetic field maximum have been found. This leads to a double humped ion-velocity spectrum, which could be interpreted in terms of a two-temperature electron distribution, in qualitative agreement with experiment.

I. INTRODUCTION

Magnetic field behavior in laser–target interactions has been a subject of great interest since the earliest suggestions of spontaneous magnetic field generation.[1,2] The presence of magnetic fields and the need for treatment of self-consistent propagation of the magnetic field laterally away from the laser spot area have led to consideration of phenomena such as thermomagnetic wave propagation[3] as well as the detailed treatment of plasma transport through mechanisms such as the Nernst effect.[4] Striking experimental results demonstrated the presence of magnetic field and the deposition of particle energy at distances far from the laser spot.[5–10] Recently, interest in laser-produced magnetic fields has developed in connection with free-electron laser concepts and laser electron acceleration.[11]

Simulations involving particle-in-cell methods,[12,13] two fluid hydrodynamic treatments,[14] and hybrid techniques[15] (with interchangeable particle and fluid plasma components) have provided substantial understanding of the lateral propagation of the magnetic field. However, results have been limited by the large disparities between time scales for electron and ion motion and between spatial scales normal to and laterally along the target surface. Phenomenological treatments[16,17] have yielded further insight into aspects of electron motion, but have not been self-consistent as concerns ion motion and electric and magnetic field variation. In addition the significance of initial conditions for the plasma at large distances from the laser spot has not been considered.

This paper aims to show the principles of magnetic field behavior, as well as a new way of solving for the plasma–magnetic field interaction beyond the laser spot. The treatment is valid for times smaller than the order of the reciprocal of the ion-cyclotron frequency at the laser spot (typically 200 psec or somewhat greater), and for laser spot sizes less than the ion gyroradius appropriate to the characteristic ion fluid velocity at the laser spot (typically of order 200 μm).

In Sec. II, we describe our physical model. In Sec. III, we write down the basic equations for coupled electron and ion fluids, then obtain asymptotically valid forms for the ion density and velocity equations and for the magnetic field. In Sec. IV, the magnetic field equation is solved in general, and the solution is specified at a fixed cylindrical radius from the laser spot center. In Sec. V, a similarity solution is found for the hydrodynamic flow equations with magnetic field. In Sec. VI, we compare our results against recent cylindrical simulations,[13] and estimate conditions under which contributions to the ion velocity spectrum from outside the laser spot are dominant over those from within. In Sec. VII, the range of validity of the solution is discussed, and its relationship to other regimes. Finally in Sec. VIII, results, as well as additional problems suggested by this work, are summarized.

II. THE MODEL

We consider the rotationally symmetric (r, z) geometry of Fig. 1, characterized by a laser beam of diameter d at the target plane, propagating along the z axis, normally incident on a flat surface. Plasma is produced in the laser spot, but in addition ions (and electrons) can leave the target at distances r ($> d/2$) from the z axis. This latter flow can be due to some unspecified mechanism such as prepulsing,[5] or through either radiation preheat or electric field breakdown,[18] which can travel along the target surface at velocities greater than $\tilde{v}_i$, the characteristic ion flow speed. Since a plasma is already present, electrons also move out beyond the laser spot at velocities greater than the ion sound speed, while the ion velocity is limited by this value. A return elec-

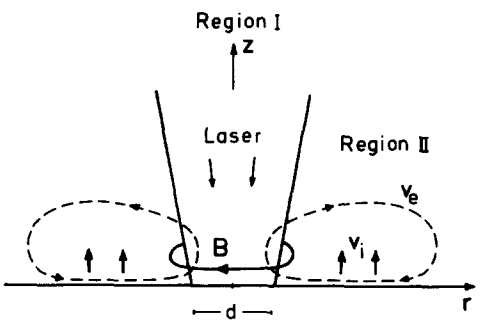

FIG. 1. Geometry indicating the laser beam, magnetic field source region (I), and outer magnetic field propagation region (II), with divergenceless electron flow and ion flow off the target surface.

[a] On leave from Los Alamos National Laboratory, Los Alamos, New Mexico 87545.

 0031-9171/87/113608-08$01.90

tron current is formed within the plasma. The total electron current generates an azimuthal magnetic field. In effect, as justified in Sec. VI, the electron velocity is sufficiently large that the electron current and the magnetic field can be determined as functions of the instantaneous spatial density. (We note that previous analytic treatments[19] involve the single-fluid approximation, which is inappropriate under these conditions.[20])

We assume an inner region (I), with $r \lesssim d/2$, within which local inhomogeneities in temperature, produced directly by the laser heating, diffuse as a result of finite ν/ω_{ce} (here ν is the electron–ion collision frequency and ω_{ce} is the electron-cyclotron frequency), and an outer collisionless, coronal region (II), with $r \gtrsim d/2$, for which $\nu/\omega_{ce} \to 0$ and T_e the electron temperature, is constant. A magnetic field is generated by the temperature (and density) gradients in region I, and propagates through region II owing to coupling with the local electron fluid.

The collisionless condition within region II is best satisfied for longer wavelength lasers which generate lower density and higher temperature coronas. The question of possible temperature structure within region II, which requires specific treatment of laser deposition and energy transport within region I as well as of heat transport within region II, has been deferred until later work. Indirectly, the increased fraction of fast-ion loss in the high laser intensity situations associated with significant magnetic field generation[8,21,22] argues for the keeping of energetic electrons in the corona. This should result in increased smoothing out of possible thermal inhomogeneities through electron return currents[23] or oscillatory electron trajectories in the corona[16] and the resulting transport of energy.

III. DERIVATION OF ASYMPTOTIC EQUATIONS

Within the assumption of quasineutrality and the neglect of electron inertia, the two-fluid equations describing the ions and electrons can be written[24] as

$$\frac{\partial n}{\partial t} + \nabla \cdot (n\mathbf{v}_i) = 0 , \tag{1}$$

$$\frac{nm_i}{Z}\left(\frac{\partial \mathbf{v}_i}{\partial t} + \mathbf{v}_i \cdot \nabla \mathbf{v}_i\right) = -\nabla p + \left(B \cdot \nabla B - \nabla \frac{B^2}{2}\right)\frac{1}{4\pi} , \tag{2}$$

$$\frac{\partial n}{\partial t} + \nabla \cdot (n\mathbf{v}_e) = 0 , \tag{3}$$

$$\nabla \times B = (4\pi/c)(\mathbf{j}_i + \mathbf{j}_e) , \tag{4}$$

$$0 = \mathbf{E} + (\mathbf{v}_e \times \mathbf{B})/c - \nabla p/nq , \tag{5}$$

$$\nabla \times \mathbf{E} = -\frac{1}{c}\frac{\partial \mathbf{B}}{\partial t} . \tag{6}$$

Here n, $\mathbf{v}_e$, and $\mathbf{j}_e$ are, respectively, the electron number density, fluid velocity, and current density, and n_i, $\mathbf{v}_i$, and $\mathbf{j}_i$ are the corresponding ion quantities, $n = Zn_i$, $\mathbf{B}$ and $\mathbf{E}$ are the magnetic and electric fields, respectively, p is the electron pressure, q is the electron charge, m_i is the ion mass, and c is the speed of light. In terms of the proton mass m_p, $m_i = Am_p$, where A is the atomic number. We are primarily interested in region II, beyond the laser spot. There, we have assumed that all pressure resides in the electrons for simplicity. Laser energy is dominantly deposited in electrons, and collisional energy exchange between electrons and ions is weak in comparison to momentum exchange, which itself is neglected. Since we assume isothermal conditions, thermal forces on the electrons vanish in Eq. (5). Frictional forces are negligible in the limit $\nu/\omega_{ce} \to 0$.

We expect the radial and axial components of ion velocity (v_{ir} and v_{iz}, respectively) to be comparable, but since the source of ions at r is the material surface in the vicinity of r, there exists a well-defined regime with

$$L_z < L_r , \tag{7}$$

where L_z and L_r are the scale lengths for variation in the respective subscripted directions. Characteristically we anticipate at time τ, $L_z \approx v_i\tau$ and $L_r \approx r$. From Eq. (1) and the z component of Eq. (2), on using (7), we readily obtain

$$\frac{\partial n}{\partial t} + \frac{\partial}{\partial z}(nv_{iz}) = 0 , \tag{8}$$

$$\frac{nm_i}{Z}\left(\frac{\partial v_{iz}}{\partial t} + v_{iz}\frac{\partial}{\partial z}v_{iz}\right) = -\frac{\partial p}{\partial z} - \frac{1}{8\pi}\frac{\partial B^2}{\partial z} . \tag{9}$$

Without loss of generality, for rotational (azimuthal) symmetry, $\mathbf{B}$ can be written in the form

$$\mathbf{B} = (4\pi/c)[\chi(r,z)/r]\hat{e}_\varphi , \tag{10}$$

and, from Eq. (4),

$$\mathbf{j} = (1/r)\nabla\chi \times \hat{e}_\varphi . \tag{11}$$

Further for

$$|v_e| > |v_i| , \tag{12}$$

we have from (11)

$$\mathbf{v}_e \simeq (1/nqr)\nabla\chi \times \hat{e}_\varphi . \tag{13}$$

Then substituting (5), (10), and (11) in (6), we obtain

$$\frac{1}{r}\frac{\partial \chi}{\partial t} = \frac{-1}{2q}\nabla\left(\frac{1}{nr^2}\right)\times\nabla\chi^2 - \frac{c^2}{4\pi q}\nabla\left(\frac{1}{n}\right)\times\nabla p . \tag{14}$$

IV. PROPAGATION, PROPERTIES, AND FORM OF MAGNETIC FIELD

Outside of the magnetic field source region $\nabla T = 0$. Using the perfect gas law $p = nT$, and $\nabla(1/n)\times\nabla p = \nabla(1/n)\times T\nabla n = 0$, so that

$$\frac{1}{r}\frac{\partial \chi}{\partial t} + \frac{1}{2q}\nabla\left(\frac{1}{nr^2}\right)\times\nabla\chi^2 = 0 , \tag{15}$$

Eq. (15) is a hyperbolic propagation equation for χ; $d\chi/dt = 0$ for trajectories such that

$$v_r = \frac{dr}{dt} = \frac{r}{q}\frac{\partial}{\partial z}\left(\frac{1}{nr^2}\right)\chi , \tag{16a}$$

$$v_z = \frac{dz}{dt} = \frac{-r}{q}\frac{\partial}{\partial r}\left(\frac{1}{nr^2}\right)\chi . \tag{16b}$$

In the source region (I), one expects that ∇n is directed in the negative z direction and ∇T in the negative r direction, so that the term in $\nabla n \times \nabla T$ in Eq. (14) results in $\chi < 0$ and $v_r > 0$, i.e., magnetic field information propagates radially outward.

For time scales of laser variation greater than r/v_r, with v_r given by Eq. (16a), subject to self-consistency conditions derived in Sec. V, one expects

$$\frac{\partial \chi}{\partial t} \simeq 0 \tag{17}$$

within Eq. (15) and

$$\nabla(1/nr^2) \times \nabla \chi^2 = 0 . \tag{18}$$

The general solution of this equation is

$$\chi = \chi(nr^2) , \tag{19}$$

and the magnetic field varies as r^{-1} provided nr^2 is constant. If $n(r,z)$ varies sufficiently weakly with radius, and if, in addition, one anticipates $\partial n/\partial z < 0$, then the value of z for which nr^2 is constant increases with increasing r. The magnetic field is in effect "pushed" further out axially into the corona with increasing r to lower electron densities.

Similarly, on defining the plasma beta as

$$\beta = 8\pi nT/B^2 , \tag{20}$$

for our isothermal case, we have

$$\beta \propto nr^2/\chi^2 . \tag{21}$$

Hence

$$\beta = \beta(nr^2) , \tag{22}$$

and the location in z of the minimum plasma beta should tend to increase with increasing r, while the actual value for the minimum beta should remain constant.

The analytic form of χ is constrained by boundary conditions. At any fixed r we anticipate that all of the radial current flow takes place in a coronal region, i.e., that there is no return current through the cold, low conductivity target material. From Eq. (4) it follows that the magnetic field is zero above some density, so that

$$\chi = 0, \quad n \geqslant n_0(r) . \tag{23}$$

This condition is satisfied when

$$\lim_{n \to n_0} \chi = [(n_0 - n)r^2]^{\alpha}, \quad \alpha > 0, \quad n < n_0 . \tag{24a}$$

In order for there to be no net radial current flow at a given radius, one finds by integration of the r component of Eq. (4) from $z(n_0)$ to larger z that there must exist some value of the electron density, $n_-(r)$ $(< n_0)$, such that $\chi(n) = 0$, $n \leqslant n_-(r)$. Since the specific value of $n_-(r)$ does not appear to be critical to the discussion below we choose the special case

$$\chi(n) = 0, \quad n = 0 ,$$

corresponding to which one can write

$$\lim_{n \to 0} \chi = (nr^2)^{\epsilon}, \quad \epsilon > 0, \quad n > 0 . \tag{24b}$$

For either $1 > \alpha > 0$ or $1 > \epsilon > 0$, there is singular behavior in $\partial \chi/\partial n$ as either $n \to 0$ or $n \to n_0$. The choice

$$\alpha = \epsilon = 1 \tag{24c}$$

in (24a) and (24b) avoids this possibility without introducing any additional zeros at $n = n_0$ or $n = 0$.

On combining Eqs. (10) and (24a)–(24c), we can write $\mathbf{B}$ in the form

$$\mathbf{B} = (4\pi/c)(nr^2)[(n_0 - n)r^2] G(nr^2) \hat{e}_{\varphi}/r ,$$

where G need have no further zeros for $n \leqslant n_0$, or equivalently

$$B^2/8\pi = n^2(n_0 - n)^2 \gamma h(n,r) ,$$

with

$$h(n,r) = G^2(nr^2)$$

and

$$\gamma = 2\pi r^6/c^2 .$$

Without loss of generality, *at fixed r*, one has

$$h(n,r) = g(n) ,$$

and hence

$$B^2/8\pi = \gamma n^2(n_0 - n)^2 g(n) \equiv \delta(n), \quad n \leqslant n_0 , \tag{25}$$

where g need have no further zeros for $n \leqslant n_0$. From Eq. (19), since $\chi(n_0 r^2) = 0$, we have

$$n_0(r) = Cr^{-2} , \tag{26}$$

where C is a constant, which can, for instance, be determined by conditions just outside the laser spot, and

$$\gamma \sim r^6 \sim n_0^{-3} . \tag{27}$$

V. SIMILARITY TREATMENT OF HYDRODYNAMIC FLOW EQUATIONS

The hydrodynamic flow behavior is defined by Eqs. (8), (9), and (25). By virtue of Eq. (25), Eq. (9) can be rewritten in the form

$$\frac{\partial v_{iz}}{\partial t} + v_{iz} \frac{\partial v_{iz}}{\partial z} = -\frac{Z}{m_i} \frac{T(n)}{n} \frac{\partial n}{\partial z} , \tag{28}$$

with

$$T(n) = T + \frac{d\delta(n)}{dn} . \tag{29}$$

Insight into the implications of the system defined by Eqs. (8) and (28) can be gained through similarity analysis.[25] With the general ansatz

$$n = N(\xi)/a^k , \tag{30a}$$

$$v_{iz} = V_i(\xi) \frac{da}{dt} , \tag{30b}$$

$$\xi = z/a(t) , \tag{30c}$$

these equations become

$$\frac{dN}{d\xi}(V_i - \xi) + N\left(\frac{dV_i}{d\xi} - k\right) = 0 , \tag{31}$$

$$\left(\frac{da}{dt}\right)^2 \frac{dV_i}{d\xi}(V_i - \xi) + a \frac{d^2 a}{dt^2} V_i + \frac{Z}{m_i}\left(T + a^k \frac{d\delta}{dN}\right) \frac{1}{N} \frac{dN}{d\xi} = 0 . \tag{32}$$

A consistent solution of (31) and (32) requires

$$k = 0, \quad a(t) = t . \tag{33}$$

(The assumption $k = 0$ is reasonable when we note that the generation of the magnetic field through a term in $\nabla n \times \nabla T$ should reach a time-asymptotic steady state for laser-generated coronas in the vicinity of the laser spot.[17] Also we take the coronal temperature to be constant in time.)

Then we find

$$V_i - \xi = \pm\left(\frac{Z}{m_i}\right)^{1/2}\left(T + \frac{d\delta}{dN}\right)^{1/2}. \tag{34}$$

On differentiating (34) with respect to ξ we have

$$\frac{dV_i}{d\xi} = 1 \pm \left(\frac{Z}{m_i}\right)^{1/2}\frac{d}{d\xi}\left(T + \frac{d\delta}{dN}\right)^{1/2},$$

or equivalently

$$\frac{dV_i}{d\xi} = 1 \pm \frac{1}{2}\left(\frac{Z}{m_i}\right)^{1/2}\frac{1}{(T + d\delta/dN)^{1/2}}\frac{d^2\delta}{dN^2}\frac{dN}{d\xi}. \tag{35a}$$

On substituting (34) and (35a) in (31), after some algebra one finds

$$\pm\left(\frac{m_i}{Z}\right)^{1/2} d\xi = \frac{-dN}{2N}\frac{1}{(T + d\delta/dN)^{1/2}} \times\left[2\left(T + \frac{d\delta}{dN}\right) \pm N\frac{d^2\delta}{dN^2}\right].$$

Since $N(\xi)$ must be finite as $\delta \to 0$ and $\xi \to \infty$, we choose the positive branch for V_i in Eq. (34), thereby obtaining

$$\left(\frac{m_i}{Z}\right)^{1/2} d\xi = -\frac{dN}{N}\left(\frac{2(T + d\delta/dN) + N\,d^2\delta/dN^2}{2(T + d\delta/dN)^{1/2}}\right). \tag{35b}$$

As an illustrative example to study the effect of the magnetic field, in keeping with the form of (27), we choose

$$g(N) = 1, \quad \gamma = 2.0T/n_0^3, \tag{36}$$

and use numerical integration to solve Eq. (35b) for $\xi \geqslant 0$ with the boundary conditions

$$N(\xi = 0) = n_0, \tag{37a}$$

$$V_i(\xi = 0) = v_0, \tag{37b}$$

where $v_0 = (ZT_0/m_i)^{1/2}$ is the isothermal sound speed. [This solution corresponds to a minimum local plasma beta ($= 8\pi nT/B^2$) of $\beta \approx 3.3$.] Profiles for the plasma density, ion velocity, and magnetic field are shown in Fig. 2 (solid curves); the dashed curves represent the solution without magnetic field, i.e., with $\gamma = 0.0$.

The primary effect of the magnetic field is the retardation of ions at densities above the density at which the magnetic field peaks, and the acceleration of ions at densities below the peak; i.e., as can be seen from Eqs. (28) and (29), a force is exerted out from the magnetic field maximum. Correspondingly, relative to the field-free solution, the ion density increases inside of the magnetic field maximum, and decreases immediately outside of the maximum. This leads to two interesting consequences, both of which are illustrated in Fig. 2.

(1) In the vicinity of the magnetic field maximum, there are more lower energy ions and fewer higher energy ions than in the field-free case.

(2) Since the ion density decreases and the ion velocity increases with increasing distance from the target, these quantities exhibit greater changes on passing through the magnetic field maximum than they do at the same location for the field-free case.

The profound effect of the magnetic field on the ion velocity spectrum is indicated in Fig. 3, which shows theoretical spectra, both with the magnetic field (solid line) and in the field-free case (dashed curve). (We assume that when the laser pulse ends, the plasma cools, and ion acceleration ceases, so that from this point on, the ion velocities are frozen.[26]) For one-dimensional expansion off the target surface through unit cross-sectional area, one can define $\tilde{N}(V_i)$ as the time-normalized number density of ions in velocity space. Then one has

$$\frac{d\tilde{N}}{dV_i} = \frac{N(V_i)}{t}\frac{dz}{dV_i} = N(V_i)\frac{d\xi}{dV_i}. \tag{38}$$

For the magnetic field-free case, using $\delta(N) = 0$, one readily obtains[27]

$$N = n_0 \exp[-(V_i - v_0)/v_0] \tag{39a}$$

and

$$\ln\left(\frac{d\tilde{N}}{dV_i}\right) = 1 - \frac{V_i}{v_0}. \tag{39b}$$

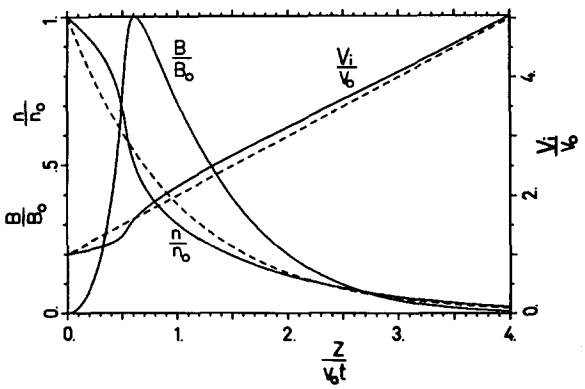

FIG. 2. Profiles for the plasma density, ion velocity, and magnetic field from the similarity solutions for $\gamma = 2.0T/n_0^3$. Both solutions with magnetic field (solid curves) and without the magnetic field (dashed curves) have the same boundary conditions: $n(\xi = 0) = n_0$, $V_i(\xi = 0) = v_0$, i.e., outflow at the isothermal sound speed at $\xi = 0$. The magnetic field normalization is $B_0 = (\pi n_0 T)^{1/2}$.

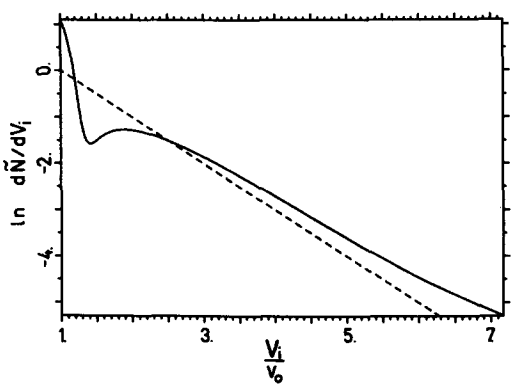

FIG. 3. Theoretical ion velocity spectra including the magnetic field (solid curve) and in the field-free case (dashed curve) with the same boundary conditions as for Fig. 2. Ion acceleration, associated with T, the constant coronal temperature during the laser pulse, ceases once the laser pulse ends.

Hence the slope of the curves has a direct interpretation in terms of the electron temperature. If one were to erroneously neglect the magnetic field, the ion spectrum in the presence of the magnetic field could be interpreted as an ion velocity distribution, driven by two spatially separate regions of differing electron temperature, even though, of course, only one temperature component is actually present. The lower velocity ions, located inside the magnetic field peak, would signify an electron temperature that is only a small fraction of the actual electron temperature, while the higher velocity ions could be associated with an electron temperature which would be slightly greater than the real electron value.

We note on using Eqs. (34) and (39a) that we can alternately write

$$N = n_0 \exp[-(z/t)(m_i/ZT)^{1/2}] . \tag{39c}$$

As the magnetic field strength increases, the terms in δ (or γ) in Eq. (35) become relatively more significant. At sufficiently large γ the quantity

$$2\left(T + \frac{d\delta}{dN}\right) + N\frac{d^2\delta}{dN^2}$$

approaches zero, and $dN/d\xi \to \infty$, i.e., discontinuities develop in N and V. At larger values of γ shocklike behavior appears likely. [For the example $g(N) = 1$, discontinuous behavior occurs at $\gamma \approx 2.7\ T/n_0^3$, with a minimum local plasma beta, $\beta \approx 2.5$.]

VI. ANALYTIC COMPARISONS

In this section, in order to demonstrate the observability of the magnetic field effects on the ion spectrum, we estimate comparative contributions to the ion velocity spectrum from ions originating inside and outside the laser spot, for low-Z targets with laser intensities (I) and wavelengths (λ) such that $I\lambda^2 > 10^{15}$ W cm^{-2} μm^2. Then we compare some result from our theory against recent simulations of magnetic field behavior in cylindrical geometry.

A. A demonstration that contributes outside the laser spot can dominate the ion velocity spectrum

As a means of estimating relative contributions to the ion, velocity spectrum, we consider the energy going into ion kinetic energy. If the ion kinetic energy dominantly resides in ions beyond the laser spot, it appears reasonable that the spectrum should be controlled by their contribution, an example of which is given by the solid curve of Fig. 3.

We begin by tracing the flow of energy in the problem. The overwhelming fraction of absorbed laser energy goes immediately into electron energy. At a given distance from the laser axis, this energy can enter other modes either through collisional deposition or through hydrodynamic transformation into a combination of ion kinetic energy and magnetic field energy.

Using $K\alpha$ emission techniques, spatially resolved collisional deposition has been determined quantitatively for a variety of target materials, laser intensities (I), and wavelengths (λ), with $I\lambda^2 > 10^{15}$ W cm^{-2} μm^2 and pulse lengths greater than or equal to 80 psec.[8] There is no case in which collisional deposition is the dominant source of energy transfer, and in which deposition at the laser spot dominates over remote deposition. Hence if ions originating in the laser spot dominate the ion-velocity spectrum, their energy source must be hydrodynamic.

We estimate the hydrodynamic transfer of energy outside the laser spot through the isothermal model, as solved for in the preceding section. For behavior in the vicinity of the laser spot, we use an isothermal model, but without the magnetic field, as has frequently been done in the past.[26] Since, as will be seen below, our calculations for ion energy for the region remote from the laser spot do not have a strong dependence on the magnetic field energy, it does not appear likely that magnetic field considerations have a significant effect on the total ion energy within the spot.

Outside the laser spot, at fixed r and t, using the solution to Eq. (35b), one may readily evaluate the electron thermal energy, ion kinetic energy, and magnetic field energy, denoted, respectively, as $E_e(r,t)$, $E_k(r,t)$, and $E_B(r,t)$:

$$E_e(r,t) = \frac{3}{2} T \int_{z_i}^{\infty} n(r,z,t)\,dz , \tag{40a}$$

$$E_k(r,t) = \frac{m_i}{2Z} \int_{z_i}^{\infty} n(r,z,t) v_{iz}^2(r,z,t)\,dz , \tag{40b}$$

$$E_B(r,t) = \frac{1}{8\pi} \int_{z_i}^{\infty} B^2(r,z,t)\,dz , \tag{40c}$$

where $z_i(r)$, the minimum axial value at which the similarity solution applies, is defined by the relation

$$n_0(r) = n[r, z_i(r)] ,$$

with $n_0(r)$ given by Eq. (26). To lowest nonvanishing order in the magnetic field strength, it is sufficient to use the solution to Eq. (35) in the limit $\delta = 0$, and one obtains

$$E_e(r,t) = \tfrac{3}{2} t n_0(r) T (ZT/m_i)^{1/2} , \tag{41a}$$

$$E_k(r,t) = \tfrac{5}{2} t n_0(r) T (ZT/m_i)^{1/2} , \tag{41b}$$

$$E_B(r,t) = \tfrac{1}{6} t n_0(r) T (ZT/m_i)^{1/2} (\gamma/\gamma^*) , \tag{41c}$$

with $\gamma^* = 2T/N_0^3$.

We now show that $Q(t)$, the ratio of ion kinetic energy inside the laser spot to ion kinetic energy outside the laser spot, is less than unity, provided the radial extent of coronal spread is much greater than the laser spot radius, at least for targets of low-Z material.

Equation (40b) is independent of magnetic field strength; hence on using it at all radii, we have

$$Q(t) = I(0, r_s)/I[r_s, r_m(t)] , \tag{42a}$$

where r_s is the laser spot radius, $r_m(t)$ is the maximum radius of lateral spread at time t, and

$$I(r_a, r_b) = \int_{r_a}^{r_b} \frac{5}{2} t(r) n_0(r) T(r) \left(\frac{ZT(r)}{m_i}\right)^{1/2} 2\pi r\,dr . \tag{42b}$$

For simplicity we take a stepped laser pulse, so that

$$t(r) = t, \quad 0 \leqslant r \leqslant r_s , \tag{43}$$

and, to account for time delays in lateral propagation,

$$t(r) = t/2, \quad r_s \leqslant r \leqslant r_m(t) . \tag{44}$$

Inside the laser spot we take $n_0(r)$ and $T(r)$ to be given by mean values so that

$$n_0(r) = n_{0s}, \quad 0 \leqslant r \leqslant r_s , \tag{45}$$

and

$$T(r) = T_s, \quad 0 \leqslant r \leqslant r_s . \tag{46}$$

Just outside the laser spot, by continuity of density, one has

$$n_0(r) r^2 \approx n_{0s} r_s^2 ,$$

and hence from Eq. (26)

$$n_0(r) \approx n_{0s} r_s^2 / r^2, \quad r_s \leqslant r \leqslant r_m(t) . \tag{47}$$

Since measurements of $K\alpha$ emission remote from the laser spot yield electron temperatures similar to those obtained from overall target modeling,[8,26] it is reasonable to take

$$T(r) = T_s, \quad r_s \leqslant r \leqslant r_m(t) . \tag{48}$$

On combining Eqs. (43)–(48) in Eq. (42a), we obtain

$$Q(t) \approx \{1/\ln[r_m(t)/r_s]\}(Z_s/Z_r)^{1/2} , \tag{49}$$

where Z_s is the mean ionic charge in the laser spot corona and Z_r is the mean charge in the corona remote from the laser spot.

The value of Z_r could be somewhat lower than Z_s, but the square root dependence of $Q(t)$ is relatively weaker than other quantities, and in addition, one expects that low-z coronal material will be fully ionized. Thus, at least with low-Z targets, one has

$$Q(t) < 1, \quad r_s \ll r_m(t) .$$

Hence, as was to be proved, for $I\lambda^2 > 10^{15}$ W cm^{-2} μm^2 and low-Z targets, the bulk of ion energy lies outside the laser focus.

B. Comparison with simulations in cylindrical geometry

We now compare some of our quantitative results with recent computor simulations for fully ionized hydrogen in cylindrical geometry, with $I\lambda^2 \approx 10^{16}$ Wcm^{-2} μm^2 and the laser spot diameter small compared to the planar target diameter[13]. We first consider the flow of absorbed energy into various energy modes, and then magnetic field behavior.

In the simulations, the absorption of laser energy is ramped up from zero to a constant value in a relatively short time. After this initial period, E_e, E_k, and E_B, integrated over the whole physical space of the problem, grow approximately linearly with time in the ratio

$$E_e : E_k : E_B :: 0.25 : 0.68 : 0.07 .$$

From the argument of Sec. VI A, the ion kinetic energy is predominantly located remotely from the laser spot. With minor modification in the argument, one reaches the same conclusion for the electron thermal energy. If one assumes the same for the magnetic field energy, we can neglect the region within the laser spot in evaluating E_e, E_k, and E_B over the physical space of the problem.

The linear variation in time in Eqs. (41a)–(41c) is similar to the linear growth in time of the same variables in the simulation. On integrating each of Eqs. (41a)–(41c) between r_s and $r_m(t)$, at any time, the spatial and temporal factors are common in all three cases, and one readily obtains for the ratio of energies over the physical space of the problem

$$E_e : E_k : E_B :: 0.36 : 0.60 : 0.04 ,$$

where we have used $\gamma = 2T/N_0^3$ in specifying the magnetic field energy.

The similarity in energy distributions indicates that the analytic modeling furnishes a reasonable approximation to the numerical simulations, although it is clear that in the simulations the distribution of energies may be affected by initial conditions and by energy transport through the mesh boundaries, and that the analytic modeling approximates the entire physical space of the problem by an isothermal rarefraction with magnetic field present.

The magnetic field behavior is similar in both cases in that outside the spot region, the simulations exhibit an approximate $1/r$ dependence, and the magnetic field has a single peak at fixed r, with field values approaching zero at upper- and lower-z values within the mesh. (The significance of deviations from zero at the mesh boundaries is unclear.) In the simulations, the effect of cylindrical geometry in comparison with Cartesian geometry is to move the magnetic field further away from the target plane with increasing distance from the laser axis, in agreement with the analytic result.

VII. RANGE OF VALIDITY

Within the assumption that $\nabla T = 0$ outside the laser spot, the self-consistency of our treatment rests on the following relations:

$$|v_i|/|v_e| < 1 , \tag{50a}$$

$$L_z/L_r < 1 , \tag{50b}$$

$$\frac{\partial \chi}{\partial t} \to 0 . \tag{50c}$$

On using

$$\frac{m_i n_i v_i^2}{2} \approx nT \quad \text{and} \quad \frac{\partial B}{\partial z} \approx \frac{4\pi n v_e q}{c} ,$$

with

$$\frac{\partial B}{\partial z} \approx \frac{\partial B}{\partial n}\frac{\partial n}{\partial z} \approx \frac{2B}{L_z}, \quad \beta = \frac{8\pi nT}{B^2}, \quad L_z \approx v_i \tau ,$$

with τ the time since the beginning of the laser pulse, one readily obtains that (50a) is equivalent to

$$\tau < \frac{2}{\omega_{ci}}\beta = \frac{2Am_pC}{\beta Z|q|B_0}\left(\frac{2r}{d}\right), \tag{51}$$

with B_0 a representative value for the magnetic field at the edge of the laser spot. Since $\beta = \beta(nr^2)$, the minimum value of β around which magnetic field effects are maximized is independent of r. Taking $\beta = 2$ and assuming a magnetic field ≈ 0.5 MG at $r \approx d/2$, we find

$$\tau \lesssim (2A/Z)(2r/d)10^{-10} \text{ sec} . \tag{52}$$

At a given value of r ($= r'$), the magnetic field solution, as given by Eqs. (15) and (19), depends on conditions at all $r \lesssim r'$. From (51) and (52) for

$$\tau > (2/\beta)Am_pc/(Z|q|B_0) = \tau^* ,$$

the treatment is no longer correct in some range of $r^*(\tau) > r > d/2$ with

$$r^*(\tau) = \tau\beta Z\,|q|B_0 d/4Am_p c\,. \tag{53}$$

For $r > r^*(\tau)$ a two-fluid treatment is necessary; for $r < r^*(\tau)$ a one-fluid treatment is adequate, and (13) is no longer valid. A matching problem exists between one- and two-fluid treatments of the plasma dynamics at $r = r^*(\tau)$. The prescription of (19) is valid for $r > r^*(\tau)$, but the conditions at $r^*(\tau)$ are not directly estimable.

Condition (50b) is the same as

$$\tau \lesssim r/v_i\,, \tag{54}$$

if we take $L_r \approx r$ and L_z as previously estimated. The condition is physically clear; we do not expect one-dimensional ion motion off the material surface over times for which the mass flow can communicate between the laser spot and the locations at radius r.

Condition (50c) can be expressed by the inequality $a/b < 1$, where

$$a = r^{-1}\frac{\partial\chi}{\partial t} \quad \text{and} \quad b = -q^{-1}\frac{\partial(nr^2)^{-1}}{\partial r}\chi\frac{\partial\chi}{\partial z}\,.$$

On using

$$n^{-1}\frac{\partial n}{\partial t} \approx \tau^{-1}, \quad n^{-1}\frac{\partial n}{\partial z} \approx L_z^{-1},$$

$$\frac{\partial(nr^2)^{-1}}{\partial r} \approx \frac{(nr^2)^{-1}}{r},$$

we readily obtain

$$\frac{a}{b} = \frac{L_z}{\tau}\,q\,\frac{nr^2}{\chi}\,.$$

In the region of strong magnetic field at each r, a/b is roughly constant provided that the ion charge state does not vary significantly. Hence using parameters just outside the laser spot,

$$a/b = \beta d/2r_i < 1\,, \tag{55}$$

where $r_i = v_i/\omega_{ci}$ and $\beta = O(1)$, i.e., this condition is equivalent to the condition that the ions be substantially unmagnetized in the laser spot.

VIII. DISCUSSION AND CONCLUSIONS

We have found an analytic solution for the two-dimensional, rotationally symmetric, time varying problem of the interaction of plasma and magnetic field in an isothermal corona at lateral locations away from the laser spot. The plasma is described by separate ion and electron velocities, with the magnitude of the electron velocity much greater than the ion velocity. Plasma expansion normal to the target surface takes place in a nonlocally determined azimuthal magnetic field. The treatment is self-consistent for sufficiently small laser spot diameter (of order the ion Larmor radius at the laser spot) and sufficiently short laser pulse durations (of order the reciprocal of the ion cyclotron frequency at the laser spot) as specified in Sec. VII. Solutions are valid above a minimum plasma beta ($=\beta_{\text{critical}}$); as this value is approached, discontinuous behavior in the particle density and velocity appears to develop.

Our treatment provides a number of salient experimental consequences for the region outside the laser spot.

(1) The magnetic field varies as r^{-1} along trajectories such that $nr^2 = \text{const}$. If n is not a strong function of radius, the locus of peak magnetic field should move to larger axial distances from the target with increasing radius.

(2) Characteristic structuring of the particle density and velocity occurs, at fixed radius, in relation to the magnetic field maximum.

(3) At least for $I\lambda^2 > 10^{15}\ \text{W cm}^{-2}\,\mu\text{m}^2$ and low-Z targets, contributions to the ion velocity spectrum are dominated by ions originating in the region outside the laser spot, provided that the radial extent of the corona is much greater than the laser spot radius. The outflow of the relatively low velocity ions at axial locations inside the magnetic field maximum is retarded, while the ion flow beyond the magnetic field maximum is accelerated. This leads to a two-component ion-velocity spectrum, similar to that produced in the absence of a magnetic field by two separate regions of differing electron temperature. The lower energy part of the ion spectrum, which would be associated with a lower electron temperature, originates in ions inside of the magnetic field maximum during the laser pulse, while the higher energy ions, which would be associated with a higher electron temperature, are located outside of the magnetic field maximum at the same time.

The r^{-1} variation in magnetic field appears to be consistent with recent experiments,[10] which also indicate that the region of field maximum moves to large axial distances from the target plane with increasing radius. Earlier work[6] found a more rapid decrease with increasing *r at fixed axial distance from the target surface*. Such observation could readily result if the magnetic field were to move to lower electron densities at larger axial distances from the target plane with increasing radius.

The spatial variation of density with magnetic field involves a relatively large gradient around the magnetic field maximum followed by shallower gradients at lower densities. There is striking similarity with experimental data,[7] which indicates the same qualitative variation. Indeed, if one were to neglect the effect of the magnetic field on ion motion, from Eq. (39c), Fig. 3 of Ref. 7 would clearly be interpreted in terms of ions accelerated by a low temperature electron distribution close to the target plane, and a higher temperature electron distribution further out, with a transition at the magnetic field maximum. Since this data applies to the edge of the laser spot, it is possible that the structure found in our solutions may also be valid at smaller radii.

In effect, we provide a second possibility for the interpretation of experimental two-component ion-velocity spectra,[21,26,28] which have previously been explained solely in terms of two electron temperatures.[26,28,29] Since the magnetic field produces the same qualitative result, it should be of interest to account for its effect on the data.

Finally we note that this work suggests a number of interesting theoretical extensions: (1) coupling of temperature sources and energy transport for determination of the coronal electron temperature field; (2) extension of solutions to the regime $\beta < \beta_{\text{critical}}$, where shocklike behavior

may develop; and (3) for problems with larger laser spot diameter and longer laser pulse duration, matching of the two-fluid solutions valid at large radii to single-fluid solutions valid at smaller radii.

ACKNOWLEDGMENTS

It is a pleasure to thank Dr. J. Meyer-ter-Vehn and other members of the Max-Planck-Institut für Quantenoptik for helpful discussions. Additional useful suggestions and insights were provided by N. Grandjouan, J. R. Sanmartin, J. Virmont, J. M. Wallace, and one referee.

This work was supported in part by the Commission of the European Communities in the framework of the Association EURATOM/IPP (SRG and RFS), and in part by the U. S. Department of Energy through the Professional Research and Teaching Leave Program at Los Alamos National Laboratory (SRG).

[1]J. A. Stamper, K. Papadopoulos, R. N. Sudan, S. O. Dean, E. A. McLean, and J. M. Dawson, Phys. Rev. Lett. **26**, 1012 (1971).
[2]D. A. Tidman, Phys. Rev. Lett. **32**, 1179 (1974); **35**, 1228 (1975); D. G. Colombant and N. K. Winsor, *ibid.* **38**, 697 (1977); C. E. Max, W. M. Manheimer, and J. J. Thomson, Phys. Fluids **21**, 128 (1978).
[3]G. J. Pert, Plasma Phys. **18**, 227 (1977); R. D. Jones, Phys. Rev. Lett. **51**, 1269 (1983).
[4]A. Nishiguchi, T. Yabe, M. G. Haines, M. Psimopoulos, and H. Takewaki, Phys. Rev. Lett. **53**, 262 (1984); A. Nishiguchi, T. Yabe, and M. G. Haines, Phys. Fluids **28**, 3683 (1985); T. Yabe and M. Hasegawa, Phys. Rev. Lett. **57**, 2667 (1986).
[5]J. A. Stamper, E. A. McLean, and B. H. Ripin, Phys. Rev. Lett. **40**, 1177 (1978).
[6]A. Raven, O. Willi, and P. T. Rumsby, Phys. Rev. Lett. **41**, 554 (1978).
[7]A. Raven, P. T. Rumsby, J. A. Stamper, O. Willi, R. Illingwirth, and R. Thareja, Appl. Phys. Lett. **35**, 526 (1979).
[8]F. Amiranoff, K. Eidmaan, R. Siegel, R. Fedosejevs, A. Maaswinkel, Y. Teng, J. D. Kilkenny, J. D. Hares, D. K. Bradley, B. J. MacGowan, and T. J. Goldsack, J. Phys. D **15**, 2463 (1982).
[9]M. A. Yates, D. B. van Hulsteyn, H. Rutkowski, G. Kyrala, and J. U. Brackbill, Phys. Rev. Lett. **49**, 1702 (1982); J. C. Kieffer, H. Pepin, M. Piché, J. P. Matte, T. W. Johnston, P. Lavigne, and F. Martin, Phys. Rev. Lett. **50**, 1054 (1983).
[10]M. D. J. Burgess, B. Luther-Davies, and K. A. Nugent, Phys. Fluids **28**, 2286 (1985).
[11]A. Loeb and S. Eliezer, Phys. Rev. Lett. **56**, 2252 (1986).
[12]D. W. Forslund and J. U. Brackbill, Phys. Rev. Lett. **48**, 1614 (1982); J. U. Brackbill and D. W. Forslund, J. Comput. Phys. **46**, 271 (1982).
[13]J. M. Wallace, J. U. Brackbill, and D. W. Forslund, J. Comput. Phys. **63**, 434 (1986).
[14]J. U. Brackbill and S. R. Goldman, Commun. Pure Appl. Math. **36**, 415 (1985); F. Amiranoff, J. U. Brackbill, D. Colombant, and N. Grandjouan, in *CECAM Workshop on Interactions and Transport in Laser-Plasma* (Université Paris-Sud, Orsay Cedex, France, 1984), p. 163.
[15]R. J. Mason and C. W. Cranfill, IEEE Trans. Plasma Sci. **14**, 45 (1986).
[16]R. Fabbro and P. Mora, Phys. Lett. A **90**, 48 (1982).
[17]J. M. Wallace, Phys. Rev. Lett. **55**, 707 (1985).
[18]F. Schwirzke, in *Laser Interaction and Related Plasma Phenomena* (Plenum, New York, 1987), Vol. 7, in press.
[19]D. Anderson, M. Bonnedal, and M. Lisak, Phys. Scr. **22**, 507 (1980); R. F. Schmalz, M. A. Liberman, and A. L. Velikovich, JETP Lett. **41**, 116 (1985).
[20]K. Miyamoto, *Plasma Physics for Nuclear Fusion* (MIT Press, Cambridge, MA, 1980).
[21]G. D. Tsakiris, K. Eidmann, R. Petsch, and R. Sigel, Phys. Rev. Lett. **46**, 1202 (1981).
[22]J. M. Kindel, C. H. Aldrich, J. V. Brackbill, D. W. Forslund, and L. Mascheroni, in *Proceedings of the Japan–U.S. Seminar on Theory and Application of Multi-Ionized Plasmas Produced by Laser and Particle Beams*, Nara, Japan, 3–7 May 1982, edited by C. Yamanaka (Osaka University, Osaka, Japan, 1982), p. 168.
[23]P. A. Jaanimagi, N. A. Ebrahim, N. H. Burnett, and C. Joshi, Appl. Phys. Lett. **38**, 734 (1981).
[24]S. I. Braginskii, in *Reviews of Plasma Physics* (translated from the Russian) (Consultants Bureau, New York, 1965), Vol. I, p. 205.
[25]L. I. Sedov, *Similarity and Dimensional Methods in Mechanics* (translated from the Russian) (Infosearch, London, 1985); J. Meyer-ter-Vehn and C. Schalk, Z. Naturforsch. Teil A **37**, 955 (1982); R. F. Schmalz and K. Eidmann, Phys. Fluids **29**, 3483 (1986).
[26]S. J. Gitomer, R. D. Jones, F. Begay, A. W. Ehler, J. F. Kephart, and R. Kristal, Phys. Fluids **29**, 2579 (1986).
[27]R. F. Schmalz, Phys. Fluids **29**, 1389 (1986).
[28]L. M. Wickens, J. E. Allen, and P. T. Rumsby, Phys. Rev. Lett. **41**, 243 (1978).
[29]B. Bezzerides, D. W. Forslund, and E. L. Lindman, Phys. Fluids **21**, 2179 (1978).